Acta Crystallographica Section F
Structural Biology and Crystallization Communications
ISSN 1744-3091

Purification and crystallization of *Vibrio fischeri* CcdB and its complexes with fragments of gyrase and CcdA

Natalie De Jonge,[a,b]* Lieven Buts,[a,b] Joris Vangelooven,[a,b] Natacha Mine,[c] Laurence Van Melderen,[c] Lode Wyns[a,b] and Remy Loris[a,b]

[a]Department of Molecular and Cellular Interactions, VIB, Pleinlaan 2, 1050 Brussels, Belgium, [b]Laboratorium voor Ultrastructuur, Vrije Universiteit Brussel, Pleinlaan 2, 1050 Brussels, Belgium, and [c]Laboratoire de Génétique des Procaryotes, Institut de Biologie et de Médecine, Université Libre de Bruxelles, Gosselies, Belgium

Correspondence e-mail: ndejonge@vub.ac.be

Received 6 February 2007
Accepted 14 March 2007

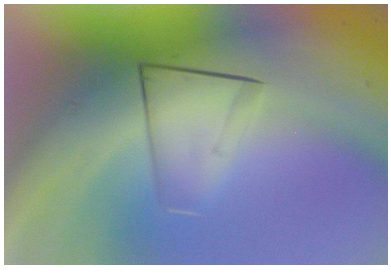

The *ccd* toxin–antitoxin module from the *Escherichia coli* F plasmid has a homologue on the *Vibrio fischeri* integron. The homologue of the toxin ($CcdB_{Vfi}$) was crystallized in two different crystal forms. The first form belongs to space group $I23$ or $I2_13$, with unit-cell parameter a = 84.5 Å, and diffracts to 1.5 Å resolution. The second crystal form belongs to space group $C2$, with unit-cell parameters a = 58.5, b = 43.6, c = 37.5 Å, β = 110.0°, and diffracts to 1.7 Å resolution. The complex of $CcdB_{Vfi}$ with the $GyrA14_{Vfi}$ fragment of *V. fischeri* gyrase crystallizes in space group $P2_12_12_1$, with unit-cell parameters a = 53.5, b = 94.6, c = 58.1 Å, and diffracts to 2.2 Å resolution. The corresponding mixed complex with *E. coli* $GyrA14_{Ec}$ crystallizes in space group $C2$, with unit-cell parameters a = 130.1, b = 90.8, c = 58.1 Å, β = 102.6°, and diffracts to 1.95 Å. Finally, a complex between $CcdB_{Vfi}$ and part of the F-plasmid antitoxin $CcdA_F$ crystallizes in space group $P2_12_12_1$, with unit-cell parameters a = 46.9, b = 62.6, c = 82.0 Å, and diffracts to 1.9 Å resolution.

1. Introduction

Toxin–antitoxin modules (TA systems) were originally discovered on low-copy-number plasmids, where their function is to stabilize the plasmid on which they are located (Ogura *et al.*, 1983). TA modules are operons that contain two genes: one encoding a toxin and one encoding an antitoxin that neutralizes the toxin. The essential key to the functionality of these systems is the difference in stability and *in vivo* half-life of the two proteins (Dao-Thi *et al.*, 2000; Van Melderen *et al.*, 1994). While the toxin is a stable protein with a long *in vivo* half-life, the antitoxin is relatively unstable and is targeted by specific proteases, reducing its *in vivo* half-life. Upon cell division, each daughter cell will inherit some of the toxin–antitoxin complexes from the cytoplasm. When a daughter cell does not inherit a copy of the plasmid, synthesis of the antitoxin is no longer possible. Antitoxin degradation will subsequently lead to liberation of the toxin. The toxin can then poison its target, leading to cell death. To date, two targets of TA toxins are known: the *ccd* and *parDE* modules target gyrase, while the more abundant *relBE*, *mazEF*, *higBA* and *yoeb*/*yefm* modules cut mRNA (for recent reviews, see Buts *et al.*, 2005; Gerdes *et al.*, 2005; Condon, 2006).

Ccd was the first TA module to be discovered and is located on the F-plasmid (Ogura & Hiraga, 1983). The antitoxin is called CcdA and the toxin CcdB. The target of the toxin is the A subunit of DNA gyrase, an essential topoisomerase of the bacterial cell (Bernard & Couturier, 1992). The crystal structures of the CcdB dimer and of a complex between CcdB and a relevant *Escherichia coli* gyrase fragment ($GyrA14_{Ec}$) are known (Loris *et al.*, 1999; Dao-Thi *et al.*, 2005). In the latter structure an important interaction is observed between Trp99 of CcdB and Arg462 of gyrase. This Trp99 is crucial for the poisoning activity of the CcdB, as proven by site-specific mutagenesis (Bahassi *et al.*, 1995).

Recently, TA modules were found to be abundant on bacterial and archaeal chromosomes (Pandey & Gerdes, 2005). Although their function is obvious on plasmids, the role of chromosomal TA systems remains highly debated (Buts *et al.*, 2005; Gerdes *et al.*, 2005; Engelberg-Kulka *et al.*, 2006). While some authors think they are

involved in a kind of altruistic cell death under conditions of nutrient stress (Aizenman *et al.*, 1996), most authors tend to believe they are stress-induced regulators that bring the cell into a kind of metabolic stasis (Christensen *et al.*, 2001). Recent evidence shows that TA systems also play a role in the emergence of persister cells (a subpopulation of the cells that are in a specific metabolic state that is temporarily not susceptible to antibiotics; Keren *et al.*, 2004; Lewis, 2005; Vazquez-Laslop *et al.*, 2006).

The *ccd* family, although the smallest of the TA families (Pandey & Gerdes, 2005), also has several chromosomal homologues (Wilbaux *et al.*, 2007). One of the most remarkable of these is present on an integron of the *Vibrio fischeri* chromosome (Rowe-Magnus *et al.*, 2003). Here, the essential Trp99 in the toxin is not conserved but is substituted by Thr103 (see Fig. 1); its interaction partner on gyrase, Arg462, is conserved in most gyrases, including that of *V. fischeri* (see Fig. 1). Mutation of Arg462 to Cys in *E. coli* gyrase provides full protection against the toxic activity of F-plasmid CcdB (Bernard & Couturier, 1992). How Thr103 of *V. fischeri* $CcdB_{Vfi}$ can take over the function of the Trp99 in F-plasmid $CcdB_F$ is unclear.

Here, we report the crystallization of $CcdB_{Vfi}$ as well as the crystallization of a complex of $CcdB_{Vfi}$ with the 36-amino-acid C-terminal half of the antitoxin from the F-plasmid ($CcdA_{F37–72}$) and the crystallization of the complexes of $CcdB_{Vfi}$ with a relevant part of the gyrases (amino acids 362–493) from *V. fischeri* ($GyrA14_{Vfi}$) and *E. coli* ($GyrA14_{Ec}$). This is the first chromosomal member of the CcdB toxin family that has been expressed, purified and crystallized.

2. Materials and methods

2.1. Cloning, expression and purification

The $ccdB_{Vfi}$ gene was amplified by the polymerase chain reaction (PCR) using plasmid p1400 (Rowe-Magnus *et al.*, 2003) as a template and using the following primers: 5′-EcoRIccdBVfi (5′-TTGTGAATTCTATGTCTCAATTTACGCTATAT-3′) and 3′-PstIccdBVfi (5′-AGTCTCTGCAGTTTAAATGCCAGTGAT-3′). The PCR product was cloned into the TOPO-XL vector (Invitrogen). The resulting plasmid was sequenced and then digested by *Eco*RI and *Pst*I. The fragment containing $ccdB_{Vfi}$ was inserted into a pKK223-3 vector opened by the same enzymes.

E. coli strain B462 harbouring the pKK223-3 plasmid with the gene for $CcdB_{Vfi}$ was grown in 2×TY medium at 310 K until an $OD_{600\,nm}$ between 0.6 and 0.8 was reached. The cells were then induced by adding 1 m*M* isopropyl β-D-thiogalactosidase (IPTG). After overnight incubation, the cells were harvested by centrifugation and subsequently resuspended in 20 m*M* Tris pH 7.0, 1 m*M* EDTA, 0.1 mg ml^{-1} 4-(2-aminoethyl)benzenesulfonyl fluoride hydrochloride (AEBSF) and 1 g ml^{-1} leupeptin. Cells were broken at 277 K by passing the cells through a cell cracker and cell debris was removed by centrifugation (30 min, 12 000*g*). The pH of the supernatant was adjusted to 7.0 with diluted HCl. The supernatant was subsequently diluted with water to lower the conductivity to 1 mS cm^{-1} prior to loading onto a Source 30Q column (Amersham Biosciences, Uppsala, Sweden). This column was eluted with a ten column-volume linear gradient of 0–0.5 *M* NaCl. The $CcdB_{Vfi}$-containing fractions were pooled and concentrated with a 0.5 kDa cutoff Vivaspin concentrator (Vivascience, Germany) prior to loading onto a Superdex 75 (16/90) size-exclusion column (run in 20 m*M* Tris pH 7.0, 1 m*M* EDTA, 150 m*M* NaCl). The eluted fractions containing $CcdB_{Vfi}$ showed essentially a single band of the correct molecular weight when analysed on SDS–PAGE.

$GyrA14_{Ec}$ was expressed and purified as described by Dao-Thi *et al.* (2004). The $gyrA14_{Vfi}$ fragment was amplified by PCR from genomic DNA from *V. fischeri* CIP103206T (kindly provided by Didier Mazel, Institut Pasteur, France) using the following primers: 5′-CCCCATATGACTCGCCGTACTATTTTTGAATTAC-3′ and 5′-CCCGGATCCTTAGCTTGCAAGAATATGCATTAGCTC-3′. The amplified fragment was digested with *Nde*I and *Bam*HI and ligated in plasmid pET15b (Novagen), which was digested with the same restriction enzymes. The vector encodes a His-tagged protein containing residues 362–493 of the $GyrA_{Vfi}$ protein with the N-terminal sequence MGSSHHHHHHSSGLVPRGSHMT, where threonine corresponds to residue 362. The plasmids were transformed in *E. coli* K514 and the nucleotide sequence was checked by DNA sequencing. The sequence-verified plasmid was amplified, purified (QIAprep Spin Miniprep Kit, Qiagen, Valencia, CA, USA) and transformed in *E. coli* BL21(DE3) for expression. Expression and purification were performed analogously as for $GyrA14_{Ec}$ (Dao-Thi *et al.*, 2004).

The C-terminal half of CcdA from *E. coli* plasmid F, $CcdA_{F37–72}$ (amino-acid sequence NH_2-RRLRAERWKAENQEGMAEVARF-IEMNGSFADENRDW-COOH), was synthesized by solid-phase synthesis by Bio-Synthesis, Lewisville, Texas, USA. The peptide was 99.14% pure as judged by HPLC analysis.

2.2. Preparation of the samples and crystallization

The $CcdB_{Vfi}$ sample was used at a concentration of 10 mg ml^{-1} in 20 m*M* Tris, 150 m*M* NaCl, 1 m*M* EDTA pH 7.0. The $CcdB_{Vfi}$–$GyrA14_{Ec}$ complex was prepared by adding concentrated $CcdB_{Vfi}$ (10 mg ml^{-1}) to a diluted solution of $GyrA14_{Ec}$ (2.8 mg ml^{-1}). After a 1 h incubation time on ice, the complex was concentrated, purified with a Superdex 75 HR 10/30 column (Amersham Biosciences) and analyzed by SDS–PAGE. The sample was used at a concentration of 7 mg ml^{-1} in 50 m*M* Tris, 150 m*M* NaCl pH 7.5. The $CcdB_{Vfi}$–$GyrA14_{Vfi}$ complex was prepared in the same way as the $CcdB_{Vfi}$–$GyrA14_{Ec}$ complex. The $CcdB_{Vfi}$–$CcdAB_{F37–72}$ complex was prepared by mixing equal volumes of 3 mg ml^{-1} $CcdB_{Vfi}$ (20 m*M* Tris pH 7.0,

```
CcdB (F plasmid)   : M-QFKVYTYK-RESR--YRLFVDVQSDIIDTPGRRMVIPLASARLLSDKVSRE
CcdB (V. fischeri): MSQFTLYKNKDKSSAKTYPYFVDVQSDLLDNLNTRLVIPLTPIELLDKKAPSH

CcdB (F plasmid)   : LYPVVHIGDESWRMMTTDMASVPVSVIGEEVADLSHRENDIKNAINLMFWGI
CcdB (V. fischeri): LCPTIHIDEGDFIMLTQQMTSVPVKILSEPVNELSTFRNEIIAAIDFLITGI


GyrA14 (E. coli)    : TRRTIFELRKARDRAHILEALAVALANIDPIIELIRHAPTPAEAKTALVANPWQLGNVAAMLERAG
GyrA14 (V. fischeri): TRRTIFELRKARDRAHILEGLALALANIDEIIELIKNAPTPAEAKEGLISRGWDLGNVASMLERAG

GyrA14 (E. coli)    : DDAARPEWLEPEFGVRDGLYYLTEQQAQAILDLRLQKLTGLEHEKLLDEYKELLDQIAELLRILGS
GyrA14 (V. fischeri): TDAARPDWLEPEFGIREGKYFLTEQQAQAILELRLHRLTGLEHEKILDEYKALLDEIAELMHILAS
```

Figure 1
Amino-acid sequence alignment of the CcdB proteins of the *E. coli* F plasmid and its *V. fischeri* chromosomal homologue and amino-acid sequence alignment of the GyrA14 fragments from *E. coli* and *V. fischeri*. Amino acids that are not conserved are indicated in red. The essential Trp99 of the F-plasmid CcdB and its equivalent Thr103 of the CcdB of *V. fischeri* are highlighted in yellow, as is the conserved Arg462 of the two gyrase fragments.

1 m*M* EDTA, 150 m*M* NaCl) and 2 mg ml^{-1} peptide (in water), followed by concentration to 10 mg ml^{-1} using a 0.5 kDa cutoff Vivaspin concentrator (Vivascience, Germany).

Initial screening of crystallization conditions was carried out with Crystal Screen, Crystal Screen II, Natrix Screen (Hampton Research) and Wizard Screen I (Emerald Biosystems) using the hanging-drop vapour-diffusion method at 293 K. Drops consisting of 2 µl protein solution and 2 µl precipitant solution were equilibrated against 500 µl precipitant solution. For the $CcdB_{Vfi}$ crystals, further optimization was carried out by varying the pH (7.0–8.0), protein concentration (8–10 mg ml^{-1}) and precipitant concentration [30–36%(*w*/*v*)PEG 1000; 1.3–1.6 *M* $LiSO_4$]. Optimization was performed using the hanging-drop vapour-diffusion technique with the same drop and reservoir volumes as used in the initial screens, except for the optimization of the $CcdB_{Vfi}$–$GyrA14_{Ec}$ complex. In this case, optimization was performed in batch mode under paraffin oil, with drops consisting of 5 µl protein solution and 5 µl precipitant solution. The protein buffer, protein concentration and temperature remained the same as in the crystal screens for all optimization experiments.

2.3. Data collection

All crystals were flash-frozen directly in the nitrogen stream. Form 2 crystals of $CcdB_{Vfi}$ were cryoprotected by enriching the precipitant solution with 32.5%(*v*/*v*) glycerol, while for form 1 crystals no additional cryoprotectant was necessary. For the $CcdB_{Vfi}$–$GyrA14_{Vfi}$ complex crystals, precipitant solution enriched with 30%(*v*/*v*) glycerol was used. Crystals of the $CcdB_{Vfi}$–$GyrA14_{Ec}$ complex were transferred stepwise to precipitant solution enriched with 25%(*v*/*v*) glycerol using 5%(*v*/*v*) steps. Crystals of the $CcdB_{Vfi}$–$CcdA_{F37–72}$ complex were cryoprotected in precipitant solution with the PEG 4000 concentration raised to 40% *via* an intermediate 27.5% step. Data were collected at 100 K on EMBL beamlines X11, X13, BW7B at the DESY synchrotron (Hamburg, Germany) and on beamline ID14-2 at the ESRF synchrotron (Grenoble, France). All data were processed using the *HKL* package (Otwinowski & Minor, 1997).

3. Results

Initial screening for crystals of $CcdB_{Vfi}$ resulted in several promising conditions. After optimization of the pH, protein concentration and the precipitant concentration, two conditions resulted in well diffracting crystals: condition 1 [50 m*M* Tris pH 7.0, 35%(*w*/*v*) PEG 400, 250 m*M* $LiSO_4$] and condition 2 [100 m*M* sodium citrate pH 5.6, 2%(*v*/*v*) polyethyleneimine, 500 m*M* NaCl]. Crystals observed in condition 1 look irregular in shape (with dimensions of 0.2 × 0.2 × 0.1 mm) and were found in drops that also contained phase separation and clusters of small needles (Fig. 2*a*). They diffracted to 1.5 Å resolution and belong to space group *I*23 or $I2_13$. The unit-cell parameter of a = 84.5 Å suggests a single subunit in the asymmetric unit, corresponding to a V_M value of 2.93 Å^3 Da^{-1}. Crystals obtained from condition 2 appear as needles with secondary growth and with a maximal length of 0.6 mm (Fig. 2*b*). They diffracted to 1.7 Å resolution and belong to space group *C*2, with unit-cell parameters a = 58.5, b = 43.6, c = 37.5 Å, β = 110.0°. Again, the asymmetric unit

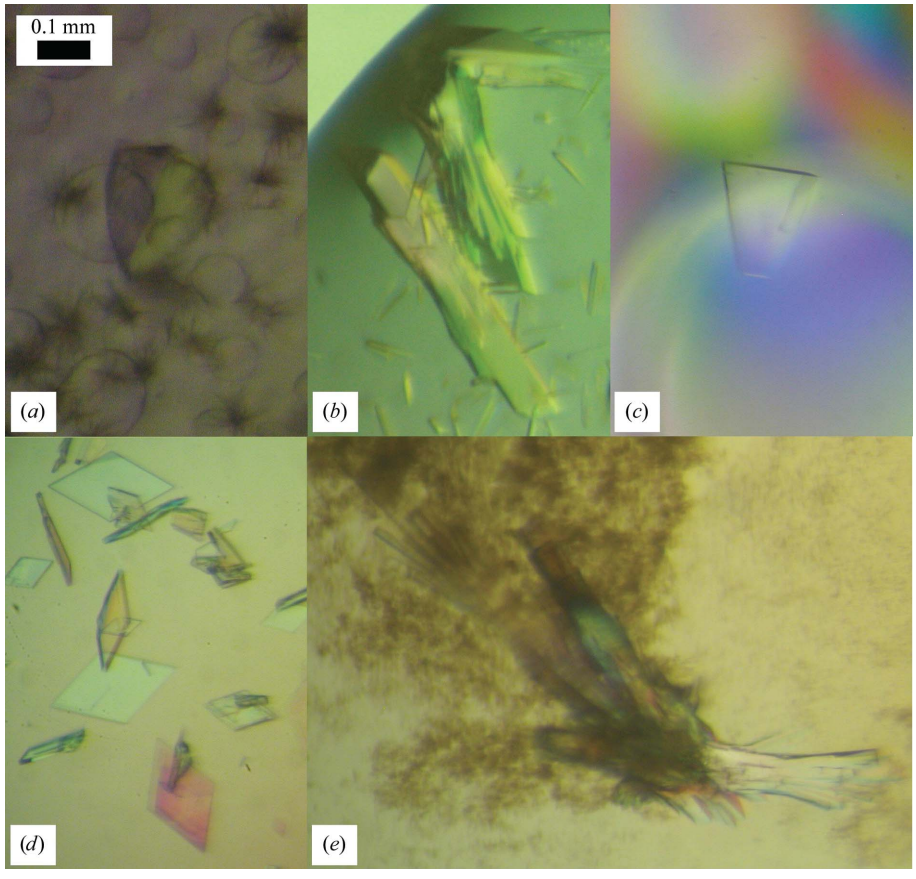

Figure 2
Crystal habits. All photographs are on the same scale, with a common scale bar shown in (*a*). (*a*) Crystal of $CcdB_{Vfi}$ (condition 1). (*b*) Crystals of $CcdB_{Vfi}$ (condition 2). (*c*) Crystals of the $CcdB_{Vfi}$–$GyrA14_{Ec}$ complex. (*d*) Crystals of the $CcdB_{Vfi}$–$GyrA14_{Vfi}$ complex. (*e*) Crystals of the $CcdB_{Vfi}$–$CcdA_{F37–72}$ complex.

Table 1
Data-collection statistics.

	$CcdB_{Vfi}$ form 1	$CcdB_{Vfi}$ form 2	$CcdB_{Vfi}$–$GyrA14_{Vfi}$	$CcdB_{Vfi}$–$GyrA14_{Ec}$	$CcdB_{Vfi}$–$CcdA_{F37–72}$
Beamline	X11 (DESY)	X11 (DESY)	BW7B (DESY)	ID14-2 (ESRF)	X13 (DESY)
Crystal-to-dector distance (mm)	125	150	250	180/340†	140
Wavelength (Å)	0.8162	0.8162	0.8423	0.9330	0.8080
No. of images	115	300	250	180	250
Angle of total revolution (°)	165	300	175	180	175
Oscillation (°)	1.0/2.0‡	1.0	0.7	1.0	0.7
Resolution (Å)	19.9–1.5 (1.55–1.50)	18.8–1.7 (1.76–1.70)	16.9–2.2 (2.28–2.20)	74.0–1.95 (2.02–1.95)	49.8–1.9 (2.00–1.90)
Space group	$I2_13$ or $I23$	$C2$	$P2_12_12_1$	$C2$	$P2_12_12_1$
Unit-cell parameters (Å, °)	$a = b = c = 84.5$	$a = 58.5$, $b = 43.6$, $c = 37.5$, $\beta = 110.0$	$a = 53.5$, $b = 94.6$, $c = 120.5$	$a = 130.1$, $b = 90.8$, $c = 58.1$, $\beta = 102.6$	$a = 46.8$, $b = 62.5$, $c = 81.9$
Completeness (%)	100.0 (100.0)	99.9 (100.0)	97.9 (94.6)	99.9 (100.0)	97.2 (91.8)
$I/\sigma(I)$	34.2 (12.186)	22.98 (8.004)	15.0 (3.112)	19.0 (9.120)	15.6 (4.070)
No. of measured reflections	306505	62778	1332994	439288	112447
No. of unique reflections	16225 (1589)	9956 (986)	29888 (2831)	48855 (4859)	18030 (1650)
R_{merge}§	0.047 (0.176)	0.040 (0.237)	0.156 (0.760)	0.050 (0.247)	0.075 (0.452)

† A low-resolution and a high-resolution pass were collected. ‡ 65 images were taken with 1° oscillation and 50 images were taken with 2° oscillation. § $R_{merge} = \sum_h \sum_i |I(h,i) - \langle I(h)\rangle| / \sum_h \sum_i I(h,i)$.

consists of a single subunit (V_M = 1.87 Å^3 Da^{-1}). Further details of the data-collection statistics are given in Table 1.

Initial screening for crystals of the $CcdB_{Vfi}$–$GyrA14_{Ec}$ complex resulted in crystals in several conditions, but the crystals were generally found to be quite fragile. Optimization of the pH (6.0–8.0) resulted in a data set for crystals grown in 50 m*M* MES pH 6.5, 1.6 *M* $(NH_4)_2SO_4$, 50 m*M* $MgCl_2$. Several cryoprotectants were tested, but good diffraction was only observed with 25%(*v*/*v*) glycerol and only when the crystals were transferred in steps of 5%(*v*/*v*) glycerol. The crystals appeared as trapezium-shaped plates (0.2 × 0.2 × 0.02 mm; Fig. 2*c*), diffracted to 1.95 Å resolution and belong to space group *C*2, with unit-cell parameters a = 130.1, b = 90.8, c = 58.1 Å, β = 102.6°. The asymmetric unit is most likely to contain a dimer of complexes, with V_M = 3.22 Å^3 Da^{-1}. The data-collection statistics are summarized in Table 1.

Small crystals were also observed for the $CcdB_{Vfi}$–$GyrA14_{Vfi}$ complex in several conditions. Optimization (by changing the ratio of NaH_2PO_4 and K_2HPO_4) finally yielded the largest crystals in 1.2 *M* NaH_2PO_4, 0.8 *M* K_2HPO_4, 100 m*M* CAPS pH 10.0. These crystals appeared as plates with dimensions of 0.1 × 0.1 × 0.02 mm (see Fig. 2*d*). They diffracted to 2.2 Å resolution and belong to space group $P2_12_12_1$, with unit-cell parameters a = 53.5, b = 94.6, c = 58.1 Å The asymmetric unit contains one complex with V_M = 2.93 Å^3 Da^{-1}. The data-collection statistics are given in Table 1.

Diffraction-quality crystals of the Ccd_{Vfi}–$CcdA_{F37–72}$ complex were obtained directly from the screen [8%(*w*/*v*) PEG 4000, 0.1 *M* $CH_3COONa{\cdot}3H_2O$ pH 4.6]. They appeared as large bundles of needles with a length of 0.8 mm (see Fig. 2*e*) and diffracted to 1.9 Å resolution. They belong to space group $P2_12_12_1$, with unit-cell parameters a = 46.9, b = 62.6, c = 82.0 Å. The asymmetric unit consists of one, or more likely two, complexes with a V_M of 5.01 or 2.5 Å^3 Da^{-1}, respectively. The data-collection statistics are listed in Table 1.

For all the complexes, it was confirmed by molecular replacement that the complex was crystallized and not the free protein.

4. Discussion

We have crystallized for the first time a chromosomal homologue from the CcdB family of toxins, $CcdB_{Vfi}$ from *V. fischeri*. $CcdB_{Vfi}$ shows 41% sequence identity to F-plasmid $CcdB_F$. Its two interaction partners, $CcdA_{Vfi}$ and $GyrA_{Vfi}$, however, show 22% and 76% sequence identity to their respective F-plasmid and *E. coli* counterparts. This is surprising as CcdA and GyrA are two competing ligands for CcdB that cannot bind simultaneously (Bernard *et al.*, 1993). In addition, one of the crucial residues of F-plasmid $CcdB_F$, Trp99, is not conserved in $CcdB_{Vfi}$ (Fig. 1). The resulting crystal structures should thus provide further insights into how recognition and specificity is achieved in the CcdB protein family.

TA systems have recently been proposed as targets for the development of new antibiotics. For example, small molecules that can interrupt the binding between the toxin and its antitoxin or small molecules that mimic the activity of the toxin might lead to bacterial cell death (Gerdes *et al.*, 2005; DeNap & Hergenrother, 2005). The structures derived from the crystals described here would help to validate such claims and aid the development of these potential small-molecule drugs. A comparison of the CcdB crystal structures of different origins and their complexes may allow the identification of the essential common elements in the CcdA–CcdB and CcdB–gyrase interactions, facilitating the development of broad host-range inhibitors.

This work was supported by grants from OZR-VUB, VIB and FWO-Vlaanderen. NDJ received a PhD fellowship from IWT and LB a post-doctoral fellowship from FWO-Vlaanderen. The authors acknowledge the use of EMBL beamlines X11, X13, BW7B (DESY, Hamburg, Germany) and ESRF beamline ID14-2 (ESRF, Grenoble, France). The authors thank Didier Mazel for providing *V. fischeri* genomic DNA and Joris Messens for discussions regarding the purification protocol for $CcdB_{Vfi}$.

References

Aizenman, E., Engelberg-Kulka, H. & Glaser, G. (1996). *Proc. Natl Acad. Sci. USA*, **93**, 6059–6063.
Bahassi, E. M., Salmon, M. A., Van Melderen, L., Bernard, P. & Couturier, M. (1995). *Mol. Microbiol.* **15**, 1031–1037.
Bernard, P. & Couturier, M. (1992). *J. Mol. Biol.* **226**, 735–745.
Bernard, P., Kezdy, K. E., Van Melderen, L., Steyaert, J., Wyns, L., Pato, M. L., Higgins, P. N. & Couturier, M. (1993). *J. Mol. Biol.* **234**, 534–541.
Buts, L., Lah, J., Dao-Thi, M.-H., Wyns, L. & Loris, R. (2005). *Trends Biochem. Sci.* **30**, 672–679.
Christensen, S. K., Mikkelsen, M., Pedersen, K. & Gerdes, K. (2001). *Proc. Natl Acad. Sci. USA*, **98**, 14328–14333.
Condon, C. (2006). *Mol. Microbiol.* **61**, 573–583.
Dao-Thi, M.-H., Messens, J., Wyns, L. & Backmann, J. (2000). *J. Mol. Biol.* **299**, 1373–1386.
Dao-Thi, M.-H., Van Melderen, L., De Genst, E., Afif, H., Buts, L., Wyns, L. & Loris, R. (2005). *J. Mol. Biol.* **348**, 1091–1102.
Dao-Thi, M.-H., Van Melderen, L., De Genst, E., Buts, L., Ranquin, A., Wyns, L. & Loris, R. (2004). *Acta Cryst.* D**60**, 1132–1134.

DeNap, J. C. & Hergenrother, P. J. (2005). *Org. Biomol. Chem.* **3**, 959–966.
Engelberg-Kulka, H., Amitai, S., Kolodkin-Gal, I. & Hazan, R. (2006). *PLoS Genet.* **2**, e135.
Gerdes, K., Christensen, S. K. & Lobner-Olesen, A. (2005). *Nature Rev. Microbiol.* **3**, 371–382.
Keren, I., Shah, D., Spoering, A., Kaldalu, N. & Lewis, K. (2004). *J. Bacteriol.* **186**, 8172–8180.
Lewis, K. (2005). *Biochemistry (Mosc.)*, **70**, 267–274.
Loris, R., Dao-Thi, M.-H., Bahassi, E. M., Van Melderen, L., Poortmans, F., Liddington, R., Couturier, M. & Wyns, L. (1999). *J. Mol. Biol.* **285**, 1667–1677.
Ogura, T. & Hiraga, S. (1983). *Proc. Natl Acad. Sci. USA*, **80**, 4784–4788.
Ogura, T., Miki, T. & Hiraga, S. (1983). *Proc. Natl Acad. Sci. USA*, **77**, 3993–3997.
Otwinowski, Z. & Minor, W. (1997). *Methods Enzymol.* **276**, 307–326.
Pandey, D. P. & Gerdes, K. (2005). *Nucleic Acids Res.* **33**, 966–976.
Rowe-Magnus, D. A., Guerout, A. M., Biskri, L., Bouige, P. & Mazel, D. (2003). *Genome Res.* **13**, 428–442.
Van Melderen, L., Bernard, B. & Couturier, M. (1994). *Mol. Microbiol.* **11**, 1151–1157.
Vazquez-Laslop, N., Lee, H. & Neyfakh, A. A. (2006). *J. Bacteriol.* **188**, 3494–3497.
Wilbaux, M., Mine, N., Guérout, A.-M., Mazel, D. & Van Melderen, L. (2007). In the press.